The EMBO Journal (2012) 31, 71–82 | © 2012 European Molecular Biology Organization | Some Rights Reserved 0261-4189/12
www.embojournal.org

THE EMBO JOURNAL

EMBO open

Cohesin acetyltransferase Esco2 is a cell viability factor and is required for cohesion in pericentric heterochromatin

Gabriela Whelan[1], Emanuel Kreidl[2,4], Gordana Wutz[2,4], Alexander Egner[3], Jan-Michael Peters[2] and Gregor Eichele[1,*]

[1]Genes and Behavior Department, Max Planck Institute for Biophysical Chemistry, Goettingen, Germany, [2]Research Institute of Molecular Pathology, Vienna, Austria and [3]Department of Nanobiophotonics, Max Planck Institute for Biophysical Chemistry, Goettingen, Germany

Sister chromatid cohesion, mediated by cohesin and regulated by Sororin, is essential for chromosome segregation. In mammalian cells, cohesion establishment and Sororin recruitment to chromatin-bound cohesin depends on the acetyltransferases Esco1 and Esco2. Mutations in Esco2 cause Roberts syndrome, a developmental disease in which mitotic chromosomes have a 'railroad' track morphology. Here, we show that Esco2 deficiency leads to termination of mouse development at pre- and post-implantation stages, indicating that Esco2 functions non-redundantly with Esco1. Esco2 is transiently expressed during S-phase when it localizes to pericentric heterochromatin (PCH). In interphase, Esco2 depletion leads to a reduction in cohesin acetylation and Sororin recruitment to chromatin. In early mitosis, Esco2 deficiency causes changes in the chromosomal localization of cohesin and its protector Sgo1. Our results suggest that Esco2 is needed for cohesin acetylation in PCH and that this modification is required for the proper distribution of cohesin on mitotic chromosomes and for centromeric cohesion.

The EMBO Journal (2012) **31,** 71–82. doi:10.1038/emboj.2011.381; Published online 18 November 2011
Subject Categories: chromatin & transcription; molecular biology of disease
Keywords: cohesin acetylation; Esco2; pericentric heterochromatin; Roberts syndrome; Sororin

Introduction

To ensure the correct transmission of genetic material, dividing cells ascertain that their chromosomes are replicated exactly once during S-phase and that the resulting two sister chromatids are held together until they are symmetrically partitioned between the daughter cells. Cohesin, a multi-subunit protein complex, plays an essential role in this process. The core subunits of cohesin, SMC1A, SMC3, RAD21/SCC1 and SCC3 form a ring-like structure that provides cohesion by tethering the sister chromatids from S-phase until metaphase (Onn *et al*, 2008; Nasmyth and Haering, 2009). In vertebrate cells, the bulk of cohesin is removed from chromosome arms in prophase (Gandhi *et al*, 2006; Kueng *et al*, 2006), except for cohesin at centromeres where it is protected from the prophase pathway by Shugoshin (SGO1) and protein phosphatase PP2A, and is maintained until the bi-orientation of chromosomes has been achieved (Sakuno and Watanabe, 2009). At the onset of anaphase, separase-mediated cleavage of the RAD21 subunit initiates a complete separation of sister chromatids, which are then pulled towards opposite poles by the mitotic spindle (Hauf *et al*, 2001; Kumada *et al*, 2006; Wirth *et al*, 2006).

Studies in yeast indicate that tethering of sister chromatids is established at the replication fork and requires the activity of Eco1 (establishment of cohesion 1) acetyltransferase, which is essential for viability in yeast (Uhlmann and Nasmyth, 1998; Skibbens *et al*, 1999; Toth *et al*, 1999; Lengronne *et al*, 2006). Eco1 acetylates K112 and K113 of Smc3 and this acetylation counteracts the anti-establishment activity mediated by the cohesin-associated proteins Rad61 and Pds5 (Ben-Shahar *et al*, 2008; Unal *et al*, 2008; Rowland *et al*, 2009; Sutani *et al*, 2009). Mammalian genomes encode two Eco1 orthologues, ESCO1 and ESCO2, that consist of a divergent N-terminus followed by a C2H2 zinc finger and a highly conserved acetyltransferase domain (Hou and Zou, 2005). In human cells, SMC3 is acetylated on K105 and K106 (Zhang *et al*, 2008), a reaction that depends on both ESCO1 and ESCO2 (Nishiyama *et al*, 2010), suggesting that these enzymes function in an at least partially redundant manner.

Partial redundancy between ESCO1 and ESCO2 may also occur in Roberts syndrome (RBS), an ESCO2 deficiency in humans that does not lead to the loss of viability (Schule *et al*, 2005; Vega *et al*, 2005). RBS patients are characterized by a series of dysmorphologies and mild-to-severe mental retardation. Most of *ESCO2* mutations introduce premature stop codons that result in truncated ESCO2 protein accompanied by a loss of the enzymatic activity (Gordillo *et al*, 2008). Metaphase preparations from RBS cells show a loss of cohesion in the pericentric heterochromatin (PCH), leading to a separation of sister chromatids at and near the centromere (Van Den Berg and Francke, 1993). In addition, RBS chromosomes exhibit a parallel alignment of sister chromatids that in combination with PCH repulsion, results in a 'railroad track' appearance of chromosomes (Maserati *et al*, 1991). These defects are particularly apparent for chromosomes 6, 7, for the acrocentrics and for the long arm of the Y chromosome (Jabs *et al*, 1991; Mannini *et al*, 2010). The molecular mechanism that causes the railroad track appearance of RBS chromosomes remains elusive and it is unclear whether this cohesion defect is solely responsible for developmental malformations observed in RBS patients (Dorsett, 2007).

*Corresponding author: Genes and Behavior Department, Max Planck Institute for Biophysical Chemistry, Am Fassberg 11, Goettingen 37077, Germany. Tel.: +49 551 201 2736; Fax: +49 551 201 2705;
E-mail: gregor.eichele@mpibpc.mpg.de
[4]These authors contributed equally to this work

Received: 15 March 2011; accepted: 22 September 2011; published online: 18 November 2011

We have generated a mouse model in which the *Esco2* gene can be conditionally inactivated by using the *Cre-loxP* system. We found that Esco2 deficiency, unexpectedly, leads to abrupt termination of development. This loss-of-cell-viability phenotype is likely caused by a defect in sister chromatid cohesion in the PCH of all chromosomes, leading to a prometaphase delay and apoptosis. We provide evidence that the railroad track appearance of chromosomes from Esco2-deficient cells reflects a specific requirement for Esco2 during the S-phase, when Esco2 protein predominantly localizes to the PCH and is required for Smc3 acetylation and Sororin recruitment. Our results implicate Esco2 in the regulation of PCH cohesion and demonstrate its non-redundant function in cohesion establishment at several cohesin-binding loci.

Results

Esco2 is required for pre-implantation development

Conditional targeting of the *Esco2* locus was achieved by inserting two *loxP* sites flanking exons 2 and 3 (Figure 1A). Upon Cre-mediated recombination, the initiation codon and the first 285 amino acids of the Esco2 protein are removed. Successful generation of conditional $Esco2^{fl/fl}$ mice was confirmed by Southern blotting (Figure 1B). To determine the *Esco2* null phenotype, $Esco2^{fl/fl}$ mice were mated with $EIIa^{CRE}$ mice expressing the Cre recombinase ubiquitously (Lakso *et al*, 1996). The *Cre* transgene was removed by backcrossing. Heterozygous mice showed no obvious phenotype, but Esco2 deficiency led to a pre-implantation loss of homozygous embryos already at the eight-cell stage (Figure 1C). We examined the mitosis of the second cell division in prometaphase-synchronized embryos and found that the anaphase of $Esco2^{-/-}$ embryos was characterized by numerous (>5) lagging chromosomes randomly scattered between two poleward-moving chromosome masses (Figure 1D). Moreover, we observed that prometaphase chromosomes isolated from two-cell stage embryos show in 20% of cells (7/36) a marked cohesion defect at the centromeres (Figure 1E). This frequency corresponds to that seen for the prevalence of $Esco2^{-/-}$ embryos at this stage and the phenotype closely resembles the one observed in Esco2-deficient MEFs ($MEFs^{Esco2\Delta/\Delta}$) (see below). We conclude that *Esco2* is required for early mouse embryogenesis and that lack of this gene causes a deficiency in cohesion.

Deletion of Esco2 in neocortical neuroepithelium leads to a premature termination of corticogenesis

The striking difference in Esco2 requirement for pre-implantation development between mouse and human led us to ask whether this difference persists in later development. We selected the developing cerebral cortex, which in mouse and human shows strong *Esco2* expression (Visel *et al*, 2007; Vega *et al*, 2010). Using the *Emx1-CRE* driver (Gorski *et al*, 2002), we deleted *Esco2* in the neuroepithelium of the dorsal telencephalon. We found that the resulting $Emx1\text{-}CRE;Esco2^{fl/fl}$ mice were viable but showed severe microcephaly (Figure 2A). $Emx1\text{-}CRE;Esco2^{fl/fl}$ embryos collected at E11.25 were characterized by a reduction in the thickness of the hippocampal primordium (unpublished observation) and at E12.5, by nearly complete agenesis of the neocortical and hippocampal neuroepithelium (Figure 2B). Adult animals lack the hippocampus and most of the cortex (Figure 2C; Supplementary Figure S1).

If sister chromatid cohesion defect is the cause of the massive loss of progenitor cells in Esco2-deficient neuroepithelium, we should observe an increase in the number of mitotic cells as a result of mitotic spindle checkpoint activation (Peters *et al*, 2008). We examined mutant E11.25 tissue with mitotic (H3S10ph) and apoptotic (TUNEL) markers and found that in comparison to wild-type, the mutant showed a nearly two-fold increase in the number of mitotic cells (Figure 2D–F). This increase was specific for the neuroepithelium of the neocortex and was not seen in the ganglionic eminence (Figure 2F), an adjacent region in which *Esco2* was not deleted. Additionally, we found that the Esco2-deficient ventricular zone (VZ) contained numerous nuclei undergoing DNA fragmentation while wild-type VZ was devoid of cell death (Figure 2G and H). Apoptotic nuclei were predominantly located in the basal part of the VZ, raising the possibility that apoptosis took place shortly after cells exited mitosis and the nuclei had translocated basally.

These data clearly demonstrate that in the absence of Esco2, the neuroepithelium ceases to grow. Thus in the mouse, Esco2 is required for pre- and post-implantation development.

Esco2 is enriched in PCH in mid-to-late S-phase nuclei

The striking cohesion defect seen in early mouse embryos and rapid loss of neuroepithelium in Esco2-deficient cortices prompted us to examine the nuclear localization of Esco2. To address this issue in a phenotype-relevant context, we selected the VZ of developing cortex, which is characterized by stereotypic nuclear movement as a result of which S-phase nuclei form a layer at the basal side of the VZ, while mitotic cells line up apically (Supplementary Figure S2A). Using this model, we were able to show that Esco2 expression sharply peaks in the S-phase (Supplementary Figure S2A and B), reminiscent of the S-phase specificity of Esco2 protein seen in MEFs (Supplementary Figure S2C), yeast (Moldovan *et al*, 2006), HeLa cells (Hou and Zou, 2005) and in RBS fibroblasts (van der Lelij *et al*, 2009).

We compared Esco2 immunofluorescence (IF) with the nuclear distribution of Pcna, that changes between early, mid and late S-phase and hence serves as a marker (Bravo and Macdonald-Bravo, 1987). Triton X-100 pre-extracted cortical sections were double-labelled for Esco2 and Pcna and analysed by confocal (Pcna) and STED (Esco2) (Hell and Wichmann, 1994) microscopy. During early S-phase, Pcna and Esco2 IF were both faint and diffuse throughout the nucleus but by mid S-phase, a striking clustering of Esco2 IF emerged (Figure 3A). In mid–late S-phase, Esco2-labelled foci became even more intense. At this stage, Esco2 IF in MEFs labelled the DAPI-dense heterochromatic foci (chromocentres), representing clusters of PCH from several chromosomes (Figure 3C, bottom row). The chromocentre core is typically marked by Hp1α IF (Quivy *et al*, 2004). Figure 3B demonstrates the localization of Esco2 IF to the Hp1α-positive region in cortical progenitor cell. Pcna marks the active sites of PCH replication that takes place at the periphery of chromocentres (ring- and horseshoe-like structures, Figure 3C). Note that Pcna IF showed virtually no overlap with Esco2 IF (Figure 3A, arrowhead).

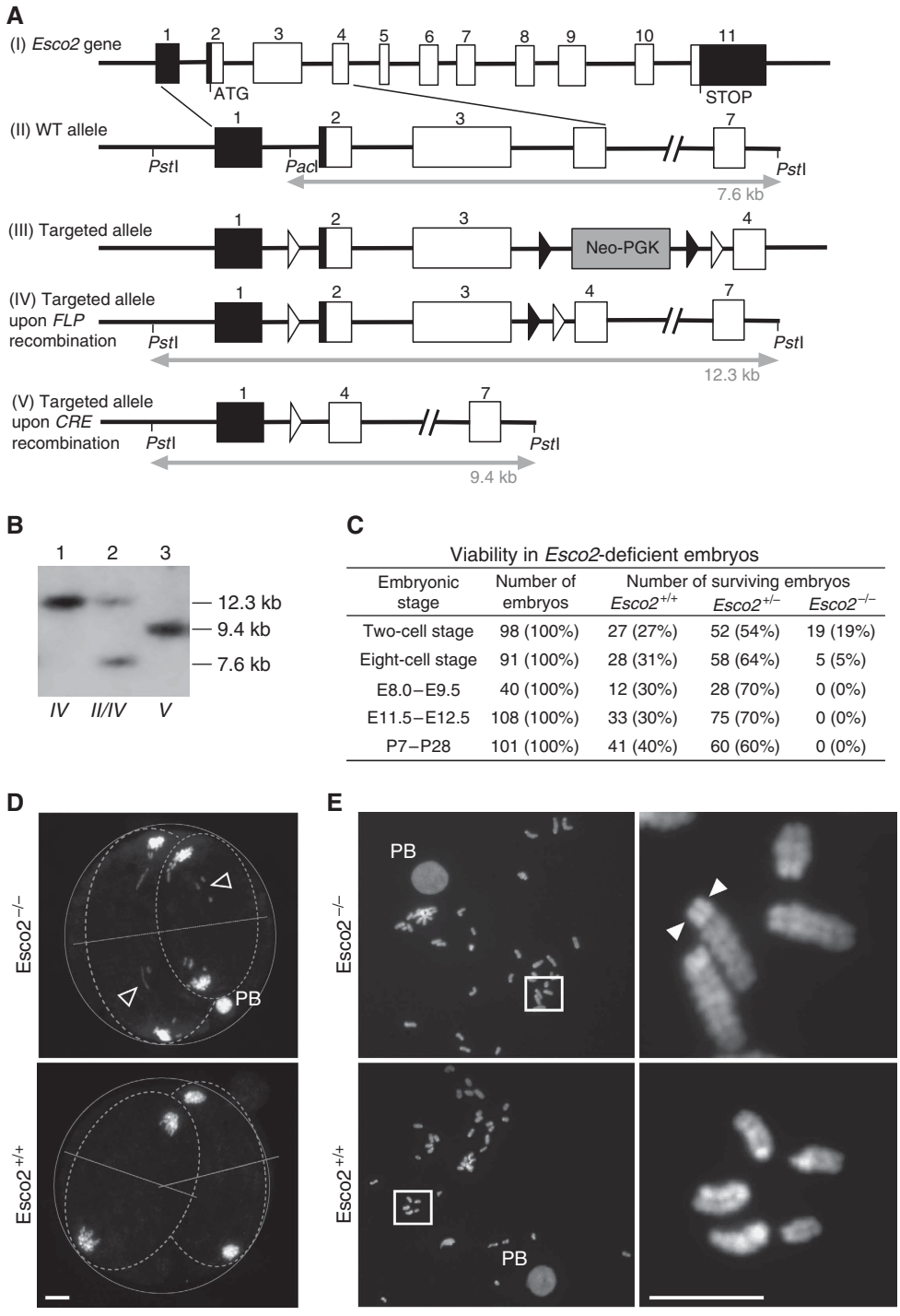

Embryonic stage	Number of embryos	Number of surviving embryos		
		Esco2$^{+/+}$	*Esco2*$^{+/-}$	*Esco2*$^{-/-}$
Two-cell stage	98 (100%)	27 (27%)	52 (54%)	19 (19%)
Eight-cell stage	91 (100%)	28 (31%)	58 (64%)	5 (5%)
E8.0–E9.5	40 (100%)	12 (30%)	28 (70%)	0 (0%)
E11.5–E12.5	108 (100%)	33 (30%)	75 (70%)	0 (0%)
P7–P28	101 (100%)	41 (40%)	60 (60%)	0 (0%)

Figure 1 Deficiency in *Esco2* leads to the termination of embryogenesis in the pre-implantation period. (**A**) *Esco2* wild-type locus (I, II), targeted allele (III–V), conditional allele prior (III) and after (IV) removal of the Neo-PGK cassette and the mutant *Esco2* allele (V) created by Cre-mediated recombination. *LoxP* and *flp* sites are marked by an empty or black triangle, respectively. (**B**) Southern blot of *Esco2* alleles following *Pac*I/*Pst*I digestion. Targeting of the *Esco2* locus leads to a loss of a *Pac*I site. Lane 1: digested genomic DNA from mice homozygous for (IV), lane 2: digested genomic DNA from mice heterozygous for (II/IV), lane 3: digested genomic DNA from mouse embryonic fibroblasts homozygous for (V). Grey arrows in (**A**) depict the restriction fragments. (**C**) *Esco2*-deficient embryos die between the two- and eight-cell stage. With development, the number of Esco2-deficient but not of heterozygous embryos decreases. *Esco2*$^{+/-}$ parents were mated. (**D**) Anaphase of two-cell stage embryos. A lagging chromosome phenotype (empty arrowheads) correlated with Esco2 deficiency. Straight lines delineate the cell division plane; the solid circle, the zona pelucida; and dashed ellipses, the cells. (**E**) In prometaphase spreads, chromosomes of mutant embryos showed loss of centromeric constriction (arrowheads). PB is the polar body. Scale bars: 5 μm. Nocodazole-synchronized embryos in (**D**, **E**) derived from heterozygous timed matings.

Next, we performed Chip-PCR with primers specific for PCH (major satellite), centromere (minor satellite), telomeres and for a several loci shown to be strongly bound by cohesin (Kagey *et al*, 2010). Chromatin from early and mid S-phase MEFs and MEFs$^{Esco2\Delta/\Delta}$ was immunoprecipitated with Esco2 antibody. Figure 4 shows high enrichment of Esco2 at PCH (characteristically bound by cohesin and histone H3K9me3). We observed only minor Esco2 binding at MmICR and Chr 11,

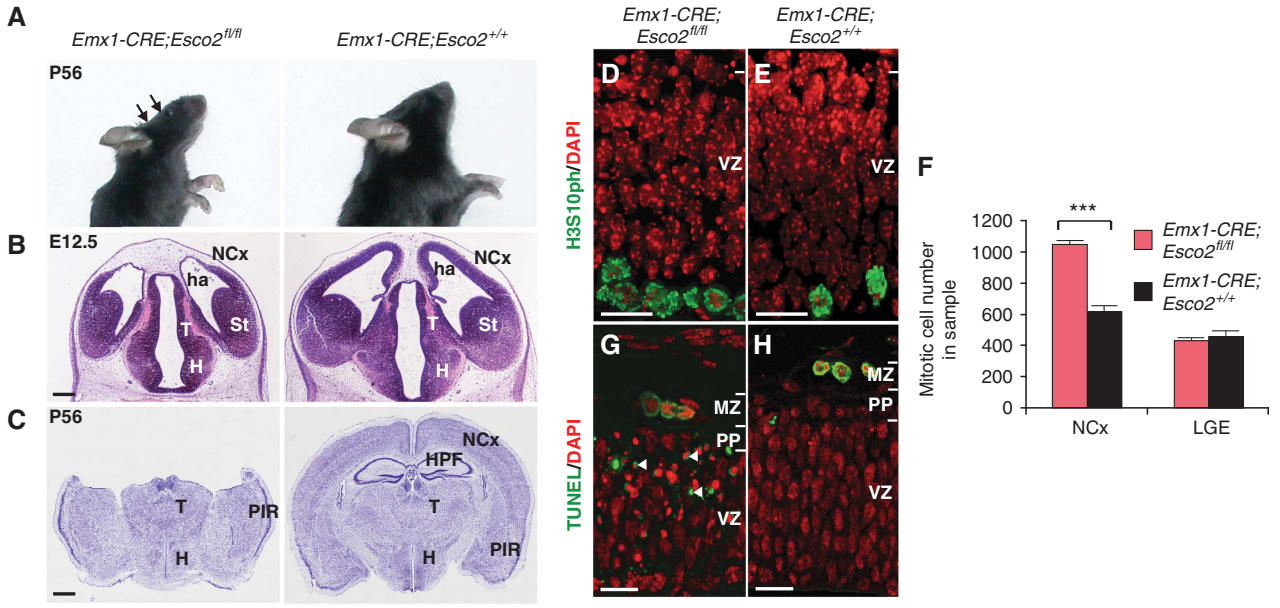

Figure 2 Deficiency in Esco2 in cortical neuronal progenitors leads to apoptosis and complete agenesis of Esco2-deficient structures. (**A**) An adult *Emx1-CRE;Esco2*$^{fl/fl}$ mouse shows severe microcephaly apparent as a flattened forehead (black arrows). (**B**) A transverse section through the mutant forebrain shows severe agenesis of hippocampal and neocortical primordia. Scale bar: 300 μm. (**C**) Coronal Nissl-stained sections reveal agenesis of the hippocampus and of most of the neocortex. Scale bar: 100 μm. (**D**, **E**) Esco2 deficiency in cortical neuroepithelium results in increased accumulation of mitotic cells at the apical side. Scale bar: 20 μm. (**F**) Total number of mitotic cells in a stack of 40 serial sections through neocortex (NCx) and lateral ganglionic eminence (LGE) regions. Mutant NCx contains nearly two times as many mitotic cells as wild-type NCx. This increase was absent in the LGE that lacks the Cre-activity (***$P<0.001$, $n=6$). (**G**, **H**) Esco2-deficient neuronal progenitors undergo apoptosis (arrowheads), which takes place predominantly basally. Scale bar: 20 μm. H, hypothalamus; ha, hippocampal anlage; HPF, hippocampal formation; MZ, marginal zone; PIR, piriform cortex; PP, preplate; St, striatum; T, thalamus.

13 and 15a loci, all of which are known to be bound by cohesin (Kagey *et al*, 2010). The absence of Esco2 binding at the centromeres and weak binding at the telomeres, which in the mouse nucleus are adjacent to the PCH, was further confirmed by IF and FISH studies (Supplementary Figure S2D–F).

We conclude that Esco2 protein levels peak in mid–late S-phase, when PCH replicates, and that the bulk of Esco2 localizes to the core region of chromocentres.

Mouse embryonic fibroblasts lacking Esco2 show severe defects in chromosome segregation

To investigate why depletion of Esco2 may lead to a delay in mitosis we analysed MEFs$^{Esco2\Delta/\Delta}$, derived from *CAGG-CRE*^{ERT}*;Esco2*$^{fl/fl}$ embryos (Hayashi and McMahon, 2002). Cre-mediated recombination was induced in the G0-arrested MEFs, which were subsequently re-arrested at the G1/S boundary by thymidine block (TB). This treatment led to nearly complete depletion of Esco2 protein (Figure 3C; Supplementary Figure S3A). MEFs$^{Esco2\Delta/\Delta}$ failed to proliferate (Supplementary Figure S3B) and showed elevated cyclin B1 levels noticeable even at 18 h after release from the TB (Supplementary Figure S3C). We also observed a nearly 2.5-fold increase in the mitotic index in asynchronously grown cultures of MEFs$^{Esco2\Delta/\Delta}$ (57 versus 24% in control MEFs). Mitotic stages were examined in synchronously grown cells 13 h after TB release. These experiments revealed that Esco2 depletion caused an approximately two-fold increase in the frequency of prometaphase/metaphase cells, while the fraction of cells in anaphase and telophase had decreased. Esco2 deficiency had little influence on the frequency of cells in prophase (Supplementary Figure S3D).

Next, we labelled mitotic cells (shaken off from synchronously progressing cultures 13 h after TB release) with mitotic spindle markers, tubulin and pericentrin. We observed that majority of mitotic MEFs$^{Esco2\Delta/\Delta}$ showed severe defects in chromosome segregation. In prometaphase/metaphase, MEFs$^{Esco2\Delta/\Delta}$ contained between one and five lagging chromosomes, which failed to bi-orient (Figure 5A). Moreover, we frequently observed cells in which several chromosomes were located near the spindle poles (Figure 5A, empty arrowheads), while the rest of them were situated at the equator. This is typical for cells in which sister chromatid cohesion had been lost in some but not all chromosomes (McGuinness *et al*, 2005). To corroborate this notion, MEFs$^{Esco2\Delta/\Delta}$ were labelled with antibodies against CenpA, a centromeric histone variant. Chromosomes containing two CenpA signals, that is, those that were composed of two sister chromatids, were frequently found at the equator, while single sister chromatids were observed near the spindle poles (Figure 5B). In other MEFs$^{Esco2\Delta/\Delta}$, likely to represent later stages of mitosis, numerous lagging chromosomes (Figure 5A, arrowheads) and chromosome bridges were seen (Figure 5A, arrows). CenpA staining indicated that lagging chromosomes were predominantly composed of single sister chromatids (Figure 5D). Chromosome bridges, however, often contained CenpA signals at both their ends near the spindle poles (Figure 5C). The chromosome bridges persisted throughout cytokinesis and were found to connect daughter cells as cytoplasmic DAPI-positive bridges in subsequent interphase

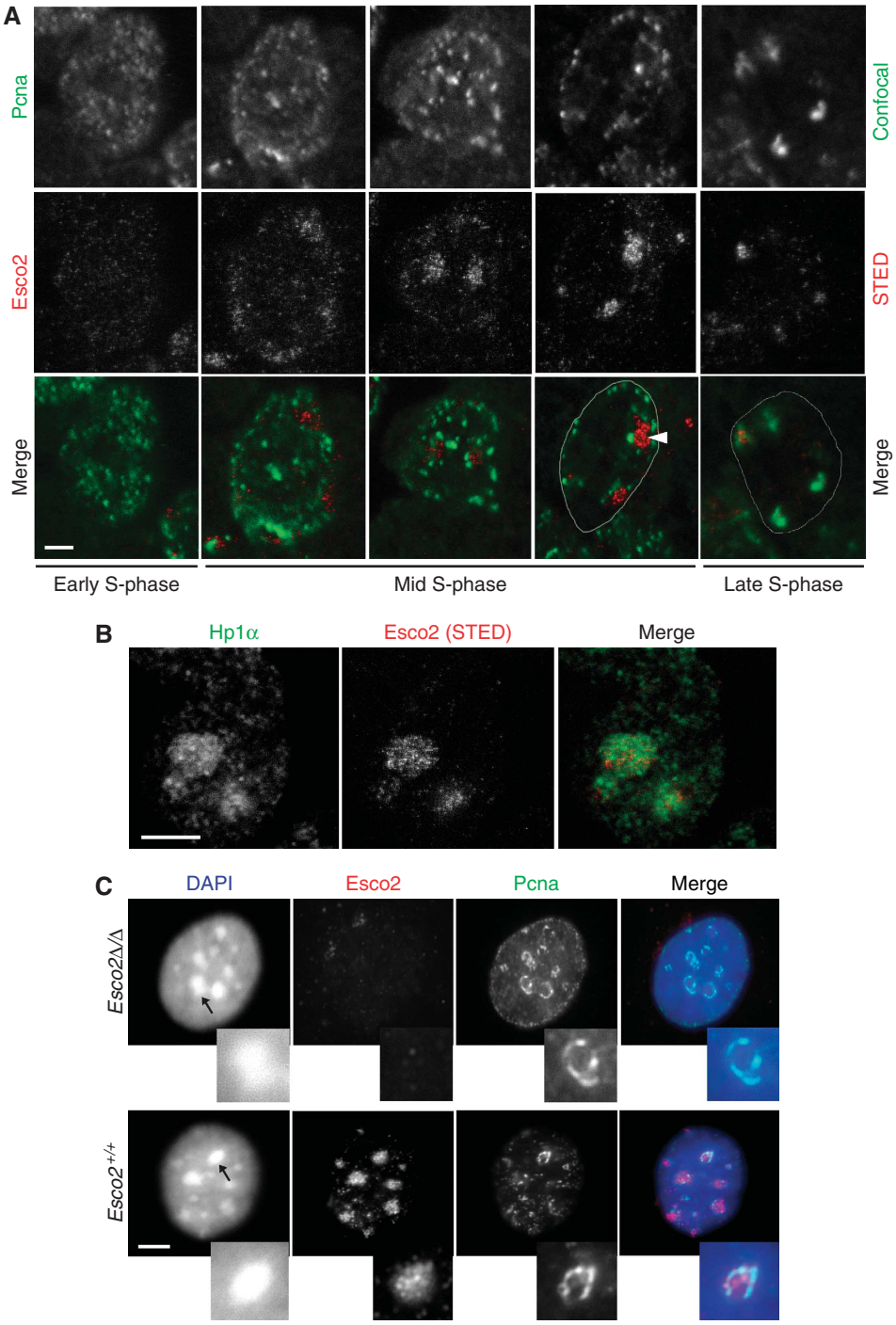

Figure 3 Esco2 is expressed during mid–late S-phase and localizes to PCH. (**A**) Confocal and STED microscopy detect Pcna and Esco2 in the nuclei of cortical neuronal progenitors. Columns 2–4 display mid S-phase nuclei characterized by patches of Pcna IF and an increase of Esco2 IF, which sharpens as the replication of PCH progresses (column 4) and results in typical Esco2 foci (arrowhead), surrounded by Pcna IF. Scale bars (**A**–**C**): 3 μm. (**B**) A high-magnification STED image reveals that Esco2 localizes to PCH as identified by Hp1α staining (confocal image). (**C**) Localization of Esco2 to the PCH in MEFs. Arrows point to individual chromocentres magnified in the insets. In wild-type cells, Esco2 localizes to the PCH core surrounded by horseshoe-like structure labelled for Pcna (bottom row). Note that Esco2-deficient MEFs lack PCH-specific Esco2 IF (top row).

(Figure 5E). This interphase was characterized by a highly abnormal nuclear morphology (Figure 5E). Apart from DAPI-positive cytoplasmic bridges, the most prominent feature was the presence of micronuclei and multilobulated nuclei (Figure 5F). The supplemental video of dividing MEFs$^{Esco2\Delta/\Delta}$ provides further evidence that the chromosomal segregation defects preceded abnormal nuclear morphology.

Prometaphase chromosomes from Esco2-deficient fibroblasts lack PCH cohesion and show reduced retention of cohesin at PCH

To test directly whether the observed chromosome segregation defects originate from abnormal sister chromatid cohesion, prometaphase chromosomes were examined. To ensure that Esco2-deficient and control MEFs had spent a

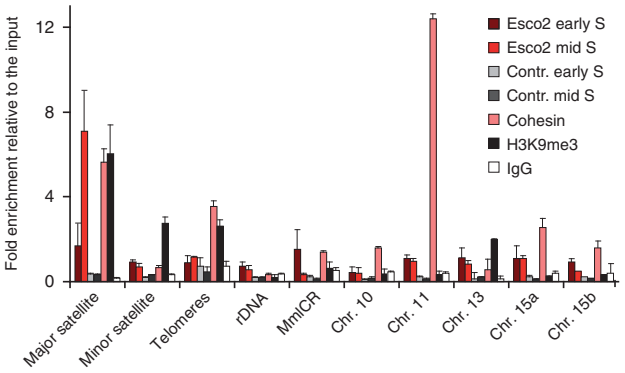

Figure 4 Chromatin immunoprecipitation reveals enrichment of Esco2 in the major satellite region and in other cohesin-bound loci located in chromosome arms. Chromatin from early and mid S-phase cells was immunoprecipitated with Esco2 antibody. Fold enrichment (relative to input) in wild-type and Esco2-deficient (control) MEFs in early and mid S-phase are shown. Since enrichment of cohesin and H3 trimethylK9 was indistinguishable in wild-type and Esco2-deficient MEFs, data are shown as single bar.

comparable time in prometaphase, mitotic cells were removed by shake-off. Remaining cells were cultured in the presence of nocodazole for 4 h and prometaphase chromosomes were prepared. Prometaphase chromosome spreads were classified into four types (Figure 6A): chromosomes in which arms and centromeres were cohered (type 1), chromosomes with cohered centromeres but loosened arms (type 2), chromosomes with cohered arms but separated centromeres (type 3, railroad track chromosomes) and single chromatids (type 4). While in the control cells, chromosomes of either type 1 or type 2 prevailed (Figure 6B), MEFs$^{Esco2\Delta/\Delta}$ chromosomes were nearly exclusively types 3 and 4, with the fraction of type 4 increasing as exposure to nocodazole was prolonged (Supplementary Figure S4B). In spreads of type 3, all chromosomes showed railroad track appearance.

The loss of pericentric cohesion in MEFs$^{Esco2\Delta/\Delta}$ prompted us to examine the localization of cohesin in prometaphase chromosomes. We used immortalized MEF$^{Esco2fl/\Delta}$ stably expressing an Myc-tagged version of Scc1 (Wirth *et al*, 2006), in which the *Esco2*$^{fl/\Delta}$ allele was deleted in logarithmically grown cells upon the infection with adenoviral Cre recombinase (AdCre). Reminiscent of our finding in primary MEFs (Supplementary Figure S3D), immortalized MEFs$^{Esco2\Delta/\Delta}$ became delayed in prometaphase/metaphase but showed no enrichment in prophase (Figure 6C). For visualization of chromatin-bound Scc1–myc, prometaphase cells were pre-extracted with Triton X-100. As expected, we observed that in control cells, Scc1–myc signal was clearly enriched at the PCH (Figure 6D, bottom right). However, in >80% of MEFs$^{Esco2\Delta/\Delta}$ (Figure 6E), Scc1–myc IF was strongly reduced in the PCH, but remained detectable in chromosome arms (Figure 6D, top right). Quantification of Scc1–myc IF intensity at the PCH relative to centromeric CREST IF intensity showed >60% reduction of the Scc1–myc IF signal in MEFs$^{Esco2\Delta/\Delta}$ (Figure 6F).

We also noticed that in MEFs$^{Esco2\Delta/\Delta}$, the distribution of Sgo1 (for specificity of anti-Sgo1 antibody see Supplementary Figure S5), Aurora B and Incenp in the prometaphase chromosomes was changed. The centromeric enrichment of these proteins readily detected in control cells (Figure 6G, right panel), was partially lost in MEFs$^{Esco2\Delta/\Delta}$ and weak fluorescence could be observed along the chromosome arms (Figure 6G, left panel; Supplementary Figure S6A–D). We investigated whether these changes could result from kinetochore defects in MEFs$^{Esco2\Delta/\Delta}$, especially because Bub1-mediated phosphorylation of histone H2A at T120 was shown to be required for proper targeting of Sgo1 to the centromeres (Kawashima *et al*, 2010). Because no antibody against mouse Bub1 or H2A pT120 is available, we examined BUB1 and H2A pT120 localization in ESCO2-depleted HeLa cells (Supplementary Figure S7A) and found that in >75% ESCO2-depleted cells, BUB1 and H2A pT120 IF at the CREST-labelled kinetochore was strongly reduced (Supplementary Figure S7B–E). Note that this reduction was not observed in control cells transfected with GL2 siRNA. Our data suggest that the increased retention of cohesin at the arms and relocalization of Sgo1 to the arms may result from defects in the kinetochore.

Depletion of Esco2 reduces acetylation of Smc3 and diminishes the amount of chromatin-bound Sororin in the entire nucleus

To address if the deficiency in Esco2 causes defects in Smc3 acetylation, we arrested MEFs containing an *Esco2*$^{fl/\Delta}$ allele in G0 and induced conversion to the *Esco2*$^{\Delta/\Delta}$ genotype by AdCre. MEFs were then released by splitting and synchronized at different stages of the cell cycle. We isolated chromatin-bound proteins and compared the ratio of Smc3 acetylated at K105/106 to total Smc3 between control and *Esco2*$^{\Delta/\Delta}$ cells by using an antibody specific for these modifications and semiquantitative western blotting. We found that Smc3 acetyl-K105/106 levels were similar in control and Esco2-deficient cells synchronized in G0 and at the G1/S transition, but Smc3 acetylation was reduced up to about 50% from mid S-phase to the early stages of mitosis (Figure 7A and B). This is consistent with the observation that Esco2 levels are highest during mid S-phase (Supplementary Figure S2A–C) and that Smc3 acetylation is linked to DNA replication (Nishiyama *et al*, 2010).

Next we determined the binding of Sororin, one of the mediators of sister chromatid cohesion, to chromatin. Sororin binding had previously been shown to depend on both cohesin and its acetylation at K105/106 (Nishiyama *et al*, 2010). Cells stably expressing LAP-tagged Sororin (Poser *et al*, 2008) were synchronized in G2 and following pre-extraction with Triton X-100 analysed by IF. Using Aurora B as a marker for G2 cells and chromocentres, we quantified GFP fluorescence at and outside the PCH in 3D (Figure 7C). We found that in control cells, Sororin was enriched at Aurora B positive foci about two-fold, similar to enrichment of Smc3 (Figure 7D; Table I). No significant signal could be detected in cells not expressing Sororin–LAP (unpublished observations). Depletion of Esco2 resulted in an over 60% reduction in chromatin-bound Sororin (Figure 7C and D) at sites of Aurora B enrichment. Levels or Aurora B as well as chromatin-bound Smc3 were not significantly altered in these cells. Sororin levels were also reduced by ~50% outside of the pericentromeric region. The IF data were further validated by Chip analyses of cells synchronized in G2. Figure 7E shows that Esco2 depletion resulted in marked reduction of PCH-bound Sororin but also in Sororin bound to another locus highly enriched for cohesin at the arm of chromosome 11 (Figure 7E). However, several cohesin-en-

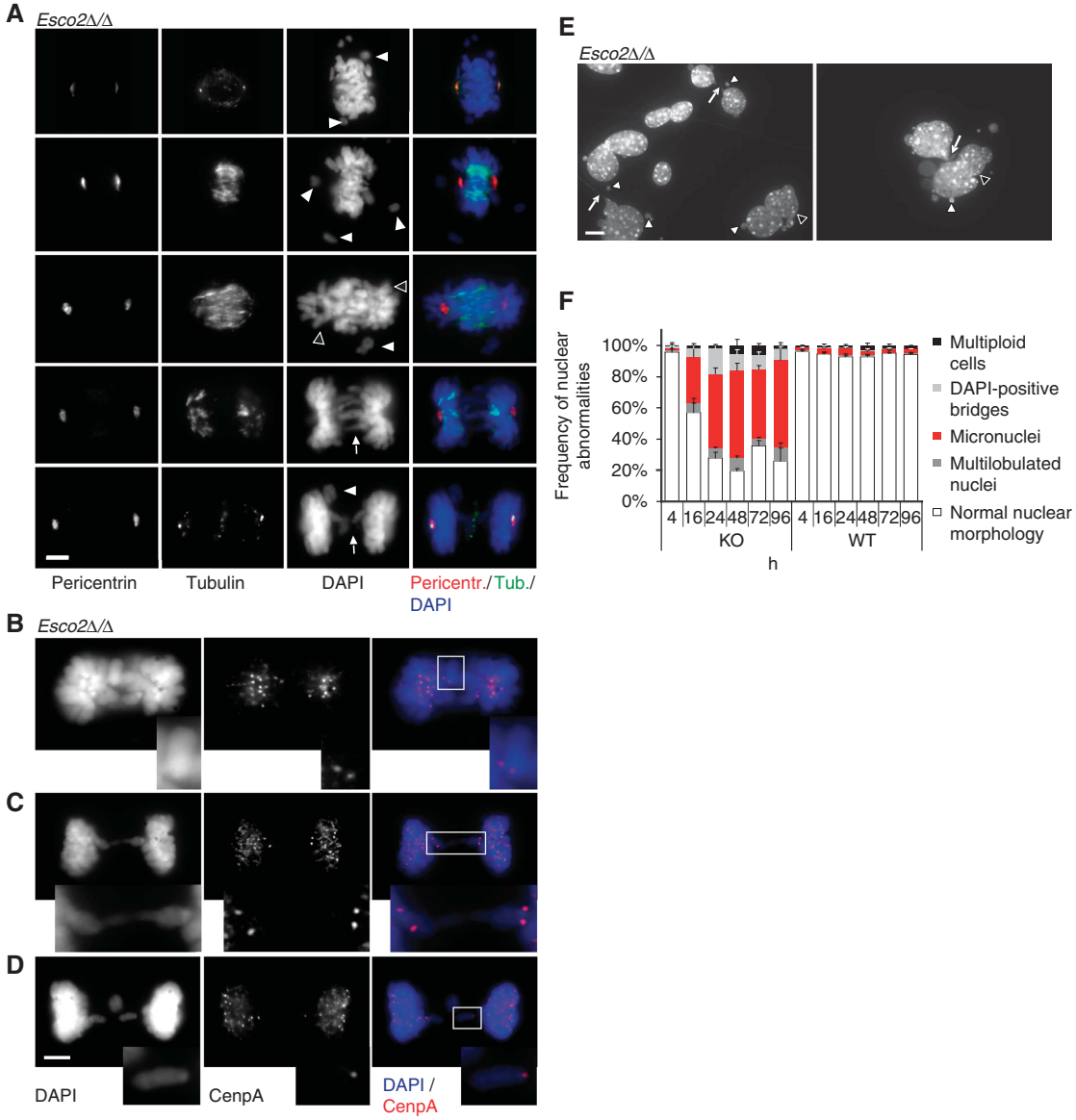

Figure 5 MEFs$^{Esco2\Delta/\Delta}$ show severe chromosome segregation defects. (**A**) Representative examples of chromosome segregation in MEFs$^{Esco2\Delta/\Delta}$ at different stages of mitosis. Images are organized in sequential order based on DNA stains and mitotic spindle morphology. Note lagging chromosomes (arrowheads), chromosomes prematurely advancing towards the spindle poles (empty arrowheads), chromosomal bridges (arrows). Scale bars (**A**–**E**): 3 μm. (**B**) A MEF$^{Esco2\Delta/\Delta}$ cell with chromosomes asynchronously advancing to the spindle poles. CenpA IF reveals that paired sister chromatids are frequently left at the equator, while single chromatids have moved to the spindle poles. Insets show the boxed area at high magnification. (**C**) Chromosomal bridges in MEFs$^{Esco2\Delta/\Delta}$ appear as a thread of DNA located in between two poleward-moving chromosomal masses. These bridges are bounded by centromeric signals. (**D**) Lagging chromosomes contain a single centromere (inset). (**E**) After exit from mitosis MEFs$^{Esco2\Delta/\Delta}$ were characterized by DAPI-positive cytoplasmic bridges (arrows), micronuclei (arrowheads) and multilobulated nuclei (empty arrowheads). (**F**) Frequency of nuclear abnormalities are shown in (**E**). Quantification was performed in regular intervals after TB release ($n > 200$ per genotype and time point).

riched loci at the chromosomes arms retained nearly normal Sororin binding in MEFs$^{Esco2\Delta/\Delta}$.

Taken together, these results indicate for the first time that Esco2 has a function in Smc3 acetylation that is not entirely redundant with the function of Esco1 or other acetyltransferases and, based on our Sororin CHIP data, suggests that depletion of Esco2 affects Smc3 acetylation levels particularly, but not only at PCH.

Discussion

It is well established that cohesin acetylation by Eco1-related acetyltransferases is required for sister chromatid cohesion (Ben-Shahar *et al*, 2008; Unal *et al*, 2008), which in turn is essential for proper chromosome segregation and cell division. However, it is unknown why mammalian cells contain two Eco1-related enzymes, Esco1 and Esco2, and why mutations of Esco2 in RBS patients lead to severe developmental defects and to the appearance of mitotic chromosomes, which lack primary constrictions at their centromeres. To begin to address these questions, we have generated a mouse model in which the Esco2 can be conditionally deleted. Our analysis of this model has revealed that Esco2 is essential for viability at different stages of mouse development and for the proper distribution of cohesin on chromosomes, that is, that Esco2 must have a function

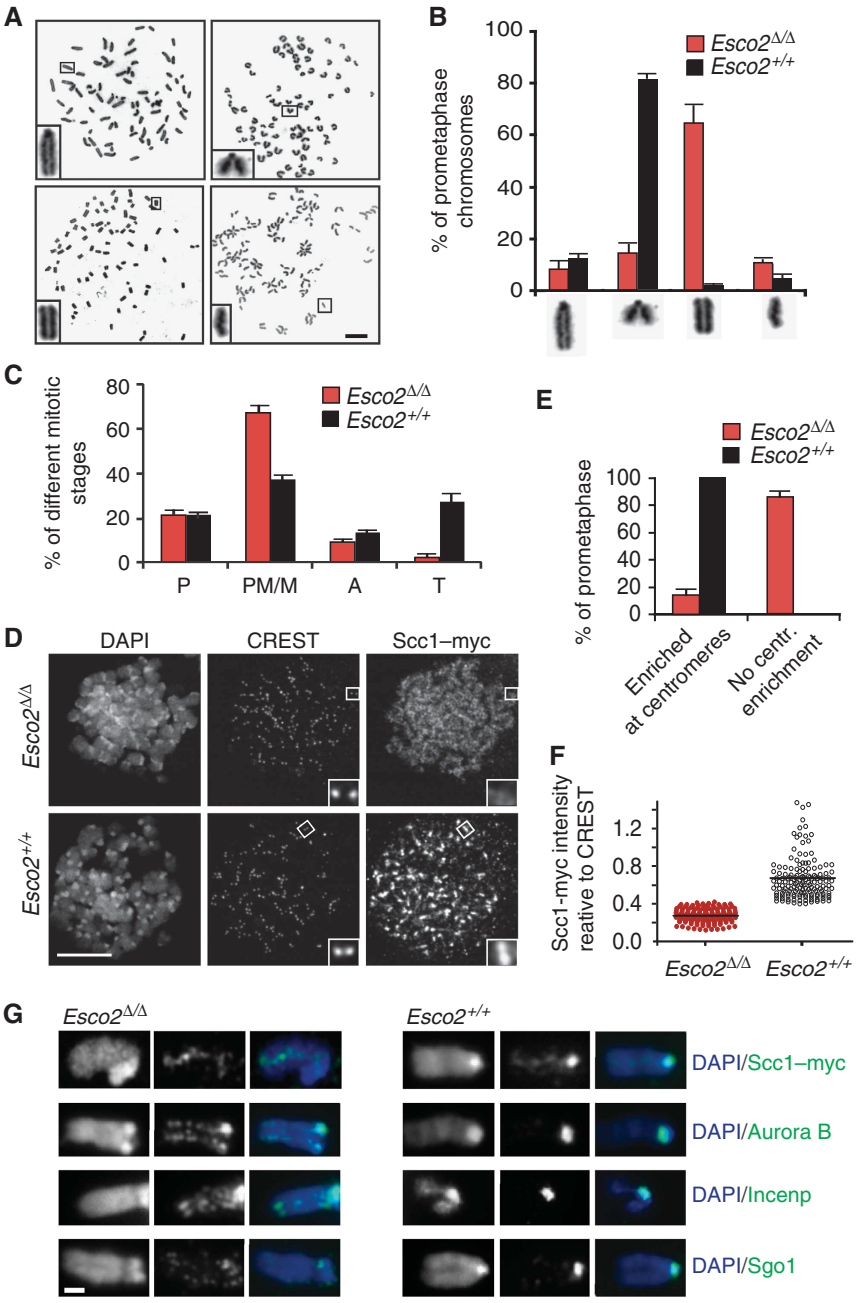

Figure 6 Esco2 deficiency leads to the railroad track appearance of chromosomes and alters the distribution of cohesin, chromosomal passenger complex and Sgo1. (**A**) Examples of prometaphase chromosomes. The two top panels display control cells, which show either type 1 or type 2 chromosomes. In MEFs$^{Esco2\Delta/\Delta}$ predominantly chromosomes of types 3 and 4 (bottom panels) were observed. Insets show a high-power view of a typical chromosome. Scale bar: 10 μm. (**B**) Frequency of different chromosome types in control MEFs and MEFs$^{Esco2\Delta/\Delta}$ after 4 h of nocodazole arrest. 70% of MEFs$^{Esco2\Delta/\Delta}$ show railroad track appearance ($n = 200$). (**C**) Esco2 deficiency leads to a delay in prometaphase/metaphase. Logarithmically grown cultures of immortalized MEFs were classified according to the DAPI stains into the different mitotic stages: A, anaphase; P, prophase; PM/M, prometaphase/metaphase; T, telophase. (**D**) Enrichment of cohesin at PCH is lost in prometaphase MEFs$^{Esco2\Delta/\Delta}$. CREST IF was used to delineate the centromere. Insets show high-power views of centromeric regions of the chromosome boxed in white. Scale bar: 10 μm. (**E**) The frequency of prometaphase cells with cohesin enriched/not enriched at the centromeres ($n = 200$). (**F**) Quantification of cohesin IF intensity at the PCH. Normalized to CREST signal intensity, MEFs$^{Esco2\Delta/\Delta}$ show a 60% reduction in cohesin signal relative to wild-type cells ($n = 200$). (**G**) Localization of cohesin, Aurora B, Incenp and Sgo1 in prometaphase chromosomes. All four proteins show strong centromeric enrichment in control cells (right panel). In MEFs$^{Esco2\Delta/\Delta}$, PCH enrichment of cohesin is lost but cohesin is seen in the arms as are Aurora B, Incenp and Sgo1 (left panel). Scale bar: 1 μm.

that can not be fulfilled by Esco1. Based on these results and our observation that Esco2 is located in PCH, we propose a model according to which Esco2 is required for acetylation of cohesin in pericentric regions, and that this modification plays an important role in mediating centromeric cohesion and allowing proper chromosome segregation.

Comparing the effect of Esco2 deficiency in humans and mice

The unexpected cell lethality observed in the absence of Esco2 at all levels from pre-implantation embryos, neuronal tissue to MEFs is in contrast to RBS studies, many of which suggest that biallelic loss of function mutations in *ESCO2* are

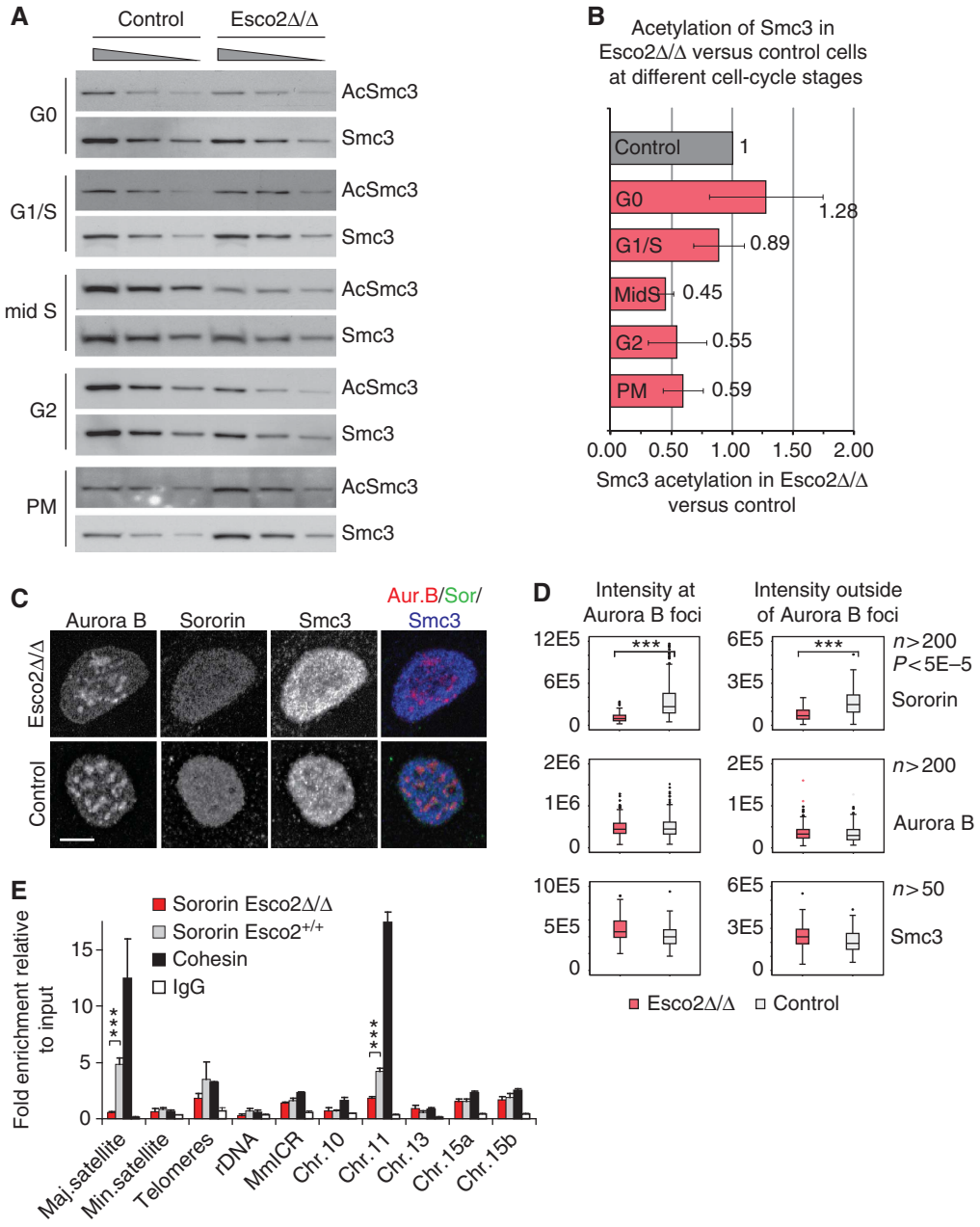

Figure 7 MEFs$^{Esco2\Delta/\Delta}$ are deficient in Smc3 acetylation and Sororin binding. (**A**) Western blots for the chromatin-bound fraction of Smc3 in control and MEFs$^{Esco2\Delta/\Delta}$ at different cell-cycle stages. Upper blot for each time point shows acetylated Smc3 while lower blot shows total Smc3. (**B**) Quantification of Smc3 acetylation levels in Esco2-depleted cells versus respective control samples as shown in (**A**). Values depict average of dilution series, error bars showing standard deviation. (**C**) IF of chromatin-bound proteins in cells depleted for Esco2 showing reduced Sororin signal throughout the nucleus. Scale bar: 5 μm. (**D**) Quantification of IF signals of Aurora B, Smc3 and Sororin in control and MEFs$^{Esco2\Delta/\Delta}$ in G2 at Aurora B positive chromocentres (left half) and outside of these (right half), showing an about 50% reduction in acetylation-dependent Sororin binding in both areas. (**E**) Chromatin immunoprecipitation of MEFs$^{Esco2\Delta/\Delta}$ reveals that Sororin binding to the major satellite (PCH) region is strongly reduced relative to control. Fold enrichment (relative to input) in G2 MEFs is shown. Note reduced Sororin binding at cohesin-bound locus in the arm of chromosome 11 (***$P<0.01$).

Table I Sororin binding to chromatin is reduced in but also outside of Aurora B positive foci

	Fluorescence intensity at Aurora B foci		Fluorescence intensity outside of Aurora B foci	
	Esco2$^{\Delta/\Delta}$	Control	Esco2$^{\Delta/\Delta}$	Control
Sororin–LAP	9590	26 611	6842	14 797
Aurora B	44 180	44 685	3272	2944
Smc3	45 921	39 900	23 946	19 245

compatible with survival into adulthood (Vega *et al*, 2010 and references therein). In addition, only ~10–20% of RBS cells show an abnormal mitosis with an anaphase characterized by one or few lagging chromosomes (Tomkins and Sisken, 1984; Jabs *et al*, 1991). MEFs$^{Esco2\Delta/\Delta}$ show premature disjunction of sister chromatids and severe mitotic defects in the form of multiple chromosome bridges and lagging chromosomes observed in nearly all cells.

We envisage two explanations for this difference. One is based on the presence of an *ESCO2* splice variant. Although the full-length ESCO2 protein was shown to be absent in RBS (Resta *et al*, 2006), these studies did not rule out the presence of the predicted shorter ESCO2 isoform, containing the zinc finger and an acetyltransferase domain and originating from an alternative spliced variant (ENSP00000380563). Future work will have to examine whether such an isoform with acetyltransferase activity indeed exists in RBS.

The second explanation involves the intrinsic difference between human and murine chromosome architecture. While in mouse, all chromosomes are acrocentics, human chromosome architecture is more diverse. Lagging chromosomes in RBS were found to be primarily C-group and smaller chromosomes (Van Den Berg and Francke, 1993), indicating that the segregation might be defective predominantly in submetacentric and acrocentric chromosomes. These chromosomes are also the ones that show heterochromatin repulsion (Petrinelli *et al*, 1984; Tomkins *et al*, 1979). In mouse, all chromosomes have this phenotype. We found that in MEFs$^{Esco2\Delta/\Delta}$ and by inference presumably also in RBS cells, cohesin instead of being enriched at PCH is partially retained in chromosome arms. In metacentric human chromosomes, this may lead to a stabilization of sister chromatid pairs on both sides of the centromere and such chromosomes might bi-orient and resist the pulling forces of the mitotic spindle more efficiently. This could ameliorate the cytogenetic phenotype of RBS, and mice with solely short acrocentric chromosomes do not benefit from this 'rescue'.

Esco2 is required for Sororin recruitment and stabilization of pericentromeric cohesin

While previous, siRNA-based studies failed to demonstrate the contribution of Esco2 to Smc3 acetylation (Zhang *et al*, 2008; Nishiyama *et al*, 2010), we show here that Smc3 acetylation is >50% reduced in MEFs$^{Esco2\Delta/\Delta}$. Smc3 acetylation had been previously associated with cohesion establishment (Rowland *et al*, 2009; Sutani *et al*, 2009). In animal cells, DNA replication and Smc3 acetylation promote the recruitment of Sororin (Lafont *et al*, 2010; Nishiyama *et al*, 2010), which through association with cohesin stabilizes the entrapment of sister chromatids in G2 (Schmitz *et al*, 2007). We found that in MEFs$^{Esco2\Delta/\Delta}$, Sororin binding was reduced to a similar extent as acetylation of Smc3. Chip analysis revealed that Sororin recruitment in Esco2-deficient cells is strongly reduced at PCH. Consistent with this finding, our IF data show that Esco2 predominantly localizes to PCH where it is highly upregulated during the mid S-phase, the time of PCH replication (Quivy *et al*, 2004; Zink, 2006). Thus, it appears that PCH might be the main site, where Esco2 mediates cohesin acetylation. Sororin recruitment to the majority of tested cohesin binding loci at the chromosome arms was not affected in MEFs$^{Esco2\Delta/\Delta}$, which raises the interesting possibility of an Esco2-independent recruitment of Sororin, possibly involving Esco1 or other acetyltransferases. Alternatively, Sororin could be recruited by other chromatin-associated protein or by direct association with DNA as proposed previously (Wu *et al*, 2010).

Consistent with >60% reduction of Sororin at PCH in G2, PCH of prometaphase chromosomes became 'unstuck' and cohesin, normally enriched at PCH in prometaphase cells, was reduced in MEFs$^{Esco2\Delta/\Delta}$. The reduction of cohesin at PCH was accompanied by partial retention of cohesin on chromosome arms. It is possible that the retention of cohesin on chromosome arms originates from changes in the kinetochore structure, which was shown to be required for proper targeting of cohesin protector Sgo1 to the centromere. Phosphorylation of H2A at T120 by Bub1 has a particular role in centromeric recruitment of Sgo1, which otherwise remains distributed along chromosome arms (Kawashima *et al*, 2010; Yamagishi *et al*, 2010). It is therefore possible that the reduction in centromeric localization of Bub1 that we have observed in >75% of ESCO2-depleted cells is the cause of increased Sgo1 levels on chromosome arms in these cells. Because Sgo1 may help to protect cohesin complexes from the prophase pathway and thus may prevent cohesin dissociation also on chromosome arms (Nakajima *et al*, 2007), the reduction in cohesin acetylation that we have observed in Esco2-deficient MEFs could, seemingly paradoxically, lead to a secondary defect—an increased persistence of cohesion between the arms of mitotic chromosomes. The 'railroad' track appearance of chromosomes in RBS cells and other cells lacking functional Esco2 may therefore not only be the consequence of reduced centromeric cohesion, but also of increased arm cohesion.

Taken together, our results suggest a first model for a specific role of Esco2 in sister chromatid cohesion that cannot be fulfilled by Esco1. According to this model, the proper establishment and maintenance of cohesion in PCH would depend on the acetylation of centromeric cohesin by Esco2, where we found Esco2 to be highly enriched around the time of DNA replication. Defects in centromere cohesion could in turn lead to structural defects in this chromosomal region that would interfere with the recruitment of Bub1 to this site, leading to the 'railroad track' appearance of the chromosomes. Whether these chromosomal defects, or perhaps other functions that Esco2 could have in the DNA damage response (Heidinger-Pauli *et al*, 2009) or in gene regulation (Dorsett, 2007; Monnich *et al*, 2011) are the cause of RBS remains to be seen.

Materials and methods

Generation of Esco2 conditional knockout mouse line

Targeting of *Esco2* locus was performed by GenOway. The *Esco2* targeting vector containing a long and a short homology arms, two *loxP* sites flanking exons 2 and 3, a FRT-flanked neomycin cassette and a Diphteria Toxin A selection marker was electroporated into the 129/SvPas ES cells. The long 5′ homology arm comprised of 5.9 kb fragment extending from an *Avr*II site to a *Bst*1107I site located in intron 1. The short 3′ homology arm contained a 1.5-kb *Bst*11007I–*Swa*I fragment spanning intron 3, exon 4 and intron 4. Neomycin-resistant ES cell clones were screened by Southern blotting and PCR. Verified ES cell clones were injected into C57BL/6J blastocysts. Resulting chimeric animals were mated with ACTB:FLPe mice ubiquitously expressing FLP recombinase (Rodriguez *et al*, 2000). Removal of the neomycin cassette and germ line transmission were validated by Southern analysis (see Supplementary data).

Generation of Esco2 and Sgo1 antisera

For rabbit and guinea pig immunization, following haemocyanin-conjugated peptides were used: peptide extending between the amino acids 10 and 70 of mouse Esco2 (guinea pig), peptide between aa 196 and 269 of mouse Esco2 (rabbit) and CTASVNY-KEPTLASKLRRGDPFT of human SGO1 (rabbit). Esco2 and SGO1 antisera were affinity purified as described (Kraft *et al*, 2003). Specificity of Sgo1 antisera was verified by IF on SGO1-depleted HeLa cells. HeLa cells were transfected with control siRNA against GL2 firefly luciferase (5′-CGUACGCGGAAUACUUCGAtt-3′), siRNAs against ESCO2 (sense 5′-CCUGCAUUGCUCUCAAUAAtt-3′ antisense 5′-UUAUUGAGAGCAAUGCAGGtt-3′) or siRNAs against SGO1 (5′-GGAUAUCACCAAUGUCUCCtt-3′) as described (Nishiyama *et al*, 2010).

Synchronization and tamoxifen-induced recombination in primary mouse embryonic fibroblasts

Single time passaged MEFs isolated from E13.5 embryos of *CAGG-Cre^{ERT};Esco2$^{fl/fl}$* or *CAGG-Cre^{ERT};Esco2$^{+/+}$* genotype were grown to confluence in DMEM containing 10% fetal bovine serum (FBS). Serum starved/contact inhibited cells were maintained in DMEM supplemented with 2% charcoal/dextran-treated FBS (PAA Laboratories) for 72 h and the conversion of floxed into the recombined allele was induced by 100 nM 4-hydroxytamoxifen. After splitting in a 1:5 ratio, cells were cultured in DMEM medium supplemented with 10% FBS and 2 mM thymidine for an additional 16 h. Cells released from TB were harvested in 3 h intervals and synchrony was assessed by IF using anti-Pcna and anti-Aurora B antibodies.

Infection with adenovirus Cre and establishment of a cell line stably expressing Scc1–myc, Esco2–LAP, Smc3–LAP and Sororin–LAP

Immortalized MEFs were cultured in DMEM supplemented with 10% FCS, 0.2 mM L-glutamine, 100 U/ml penicillin, 100 μg/ml streptomycin, 1 mM sodium pyruvate, 0.1 mM 2-mercaptoethanol and non-essential amino acids. For infection, cells were grown to 30–50% confluency, washed with PBS and infected with 7000 virus particles/cell in DMEM supplemented with 2% FCS. After 24 h, cells were transferred to fresh medium. AdCre and adenovirus expressing EGFP (Ad5 CMV Cre and EGFP) were purchased from the University of Iowa (Iowa City, IA). MEF$^{Esco2flox/\Delta}$ cell line stably expressing Scc1 was generated as described (Wirth *et al*, 2006), using murine Scc1 that was COOH-terminally tagged with nine myc epitopes inserted into *pREVTRE* vector (Clontech).

LAP-tagged Sororin was generated as described previously (Poser *et al*, 2008). Immortalized MEFs$^{Esco2fl/\Delta}$ transfected with the constructs were selected for stable integration using the neomycin selection and FACS sorting.

Supplementary data

Supplementary data are available at *The EMBO Journal* Online (http://www.embojournal.org).

Acknowledgements

We thank S Thiel, K Kiel, K Scherf, M Brockmeyer and F Grabbe for technical assistance; E Watrin, S Hauf, K Shirahige, A Kromminga and Y Watanabe for antibodies; R Ladurner for Sgo1 RNAi; and P Pasierbek and T Lendl for performing automated image analysis. The research leading to these results has received funding from the Max Planck Society, Boehringer Ingelheim, the Austrian Science Fund (FWF; special research programme SFB F34 'Chromosome Dynamics'), the Vienna Science and Technology Fund (WWTF NS09-13), the Austrian Ministry for Science and Research (GEN-AU programme 'Epigenetic control') and the European Community's Seventh Framework Programme (FP7/2007-2013) under grant agreement n° 241548 (MitoSys).

Author contributions: GW[1], EK and GW[3] designed and performed the experiments; AE, J-MP and GE supervised the experiments; GW[1], J-MP and GE wrote the manuscript with input from EK and GW[3]. All authors contributed to the editing of the manuscript

Conflict of interest

The authors declare that they have no conflict of interest

References

Ben-Shahar TR, Heeger S, Lehane C, East P, Flynn H, Skehel M, Uhlmann F (2008) Eco1-dependent cohesin acetylation during establishment of sister chromatid cohesion. *Science* **321:** 563–566

Bravo R, Macdonald-Bravo H (1987) Existence of two populations of cyclin/proliferating cell nuclear antigen during the cell cycle: association with DNA replication sites. *J Cell Biol* **105:** 1549–1554

Dorsett D (2007) Roles of the sister chromatid cohesion apparatus in gene expression, development, and human syndromes. *Chromosoma* **116:** 1–13

Gandhi R, Gillespie PJ, Hirano T (2006) Human Wapl is a cohesin-binding protein that promotes sister-chromatid resolution in mitotic prophase. *Curr Biol* **16:** 2406–2417

Gordillo M, Vega H, Trainer AH, Hou F, Sakai N, Luque R, Kayserili H, Basaran S, Skovby F, Hennekam RCM, Uzielli MLG, Schnur RE, Manouvrier S, Chang S, Blair E, Hurst JA, Forzano F, Meins M, Simola KOJ, Raas-Rothschild A *et al* (2008) The molecular mechanism underlying Roberts syndrome involves loss of ESCO2 acetyltransferase activity. *Hum Mol Genet* **17:** 2172–2180

Gorski JA, Talley T, Qiu M, Puelles L, Rubenstein JL, Jones KR (2002) Cortical excitatory neurons and glia, but not GABAergic neurons, are produced in the Emx1-expressing lineage. *J Neurosci* **22:** 6309–6314

Hauf S, Waizenegger IC, Peters JM (2001) Cohesin cleavage by separase required for anaphase and cytokinesis in human cells. *Science* **293:** 1320–1323

Hayashi S, McMahon AP (2002) Efficient recombination in diverse tissues by a tamoxifen-inducible form of Cre: a tool for temporally regulated gene activation/inactivation in the mouse. *Dev Biol* **244:** 305–318

Heidinger-Pauli JM, Unal E, Koshland D (2009) Distinct targets of the Eco1 acetyltransferase modulate cohesion in S phase and in response to DNA damage. *Mol Cell* **34:** 311–321

Hell SW, Wichmann J (1994) Breaking the diffraction resolution limit by stimulated emission: stimulated-emission-depletion fluorescence microscopy. *Opt Lett* **19:** 780–782

Hou FJ, Zou H (2005) Two human orthologues of Eco1/Ctf7 acetyltransferases are both required for proper sister-chromatid cohesion. *Mol Biol Cell* **16:** 3908–3918

Jabs EW, Tuckmuller CM, Cusano R, Rattner JB (1991) Studies of mitotic and centromeric abnormalities in Roberts syndrome—implications for a defect in the mitotic mechanism. *Chromosoma* **100:** 251–261

Kagey MH, Newman JJ, Bilodeau S, Zhan Y, Orlando DA, van Berkum NL, Ebmeier CC, Goossens J, Rahl PB, Levine SS, Taatjes DJ, Dekker J, Young RA (2010) Mediator and cohesin connect gene expression and chromatin architecture. *Nature* **467:** 430–435

Kawashima SA, Yamagishi Y, Honda T, Ishiguro K, Watanabe Y (2010) Phosphorylation of H2A by Bub1 prevents chromosomal instability through localizing shugoshin. *Science* **327:** 172–177

Kraft C, Herzog F, Gieffers C, Mechtler K, Hagting A, Pines J, Peters JM (2003) Mitotic regulation of the human anaphase-promoting complex by phosphorylation. *EMBO J* **22:** 6598–6609

Kueng S, Hegemann B, Peters BH, Lipp JJ, Schleiffer A, Mechtler K, Peters JM (2006) Wapl controls the dynamic association of cohesin with chromatin. *Cell* **127:** 955–967

Kumada K, Yao R, Kawaguchi T, Karasawa M, Hoshikawa Y, Ichikawa K, Sugitani Y, Imoto I, Inazawa J, Sugawara M, Yanagida M, Noda T (2006) The selective continued linkage of centromeres from mitosis to interphase in the absence of mammalian separase. *J Cell Biol* **172:** 835–846

Lafont AL, Song J, Rankin S (2010) Sororin cooperates with the acetyltransferase Eco2 to ensure DNA replication-dependent sister chromatid cohesion. *Proc Natl Acad Sci USA* **107:** 20364–20369

Lakso M, Pichel JG, Gorman JR, Sauer B, Okamoto Y, Lee E, Alt FW, Westphal H (1996) Efficient *in vivo* manipulation of mouse genomic sequences at the zygote stage. *Proc Natl Acad Sci USA* **93:** 5860–5865

Lengronne A, McIntyre J, Katou Y, Kanoh Y, Hopfner KP, Shirahige K, Uhlmann F (2006) Establishment of sister chromatid cohesion at the S cerevisiae replication fork. *Mol Cell* **23:** 787–799

Mannini L, Menga S, Musio A (2010) The expanding universe of cohesin functions: a new genome stability caretaker involved in human disease and cancer. *Hum Mutat* **31:** 623–630

Maserati E, Pasquali F, Zuffardi O, Buttitta P, Cuoco C, Defant G, Gimelli G, Fraccaro M (1991) Roberts syndrome—phenotypic variation, cytogenetic definition and heterozygote detection. *Ann Genet* **34:** 239–246

McGuinness BE, Hirota T, Kudo NR, Peters JM, Nasmyth K (2005) Shugoshin prevents dissociation of cohesin from centromeres during mitosis in vertebrate cells. *PLoS Biol* **3:** e86

Moldovan GL, Pfander B, Jentsch S (2006) PCNA controls establishment of sister chromatid cohesion during S phase. *Mol Cell* **23:** 723–732

Monnich M, Kuriger Z, Print CG, Horsfield JA (2011) A zebrafish model of Roberts syndrome reveals that Esco2 depletion interferes with development by disrupting the cell cycle. *PLoS One* **6:** e20051

Nakajima M, Kumada K, Hatakeyama K, Noda T, Peters JM, Hirota T (2007) The complete removal of cohesin from chromosome arms depends on separase. *J Cell Sci* **120:** 4188–4196

Nasmyth K, Haering CH (2009) Cohesin: its roles and mechanisms. *Annu Rev Genet* **43:** 525–558

Nishiyama T, Ladurner R, Schmitz J, Kreidl E, Schleiffer A, Bhaskara V, Bando M, Shirahige K, Hyman AA, Mechtler K, Peters JM (2010) Sororin mediates sister chromatid cohesion by antagonizing Wapl. *Cell* **143:** 737–749

Onn I, Heidinger-Pauli JM, Guacci V, Unal E, Koshland DE (2008) Sister chromatid cohesion: a simple concept with a complex reality. *Annu Rev Cell Dev Biol* **24:** 105–129

Peters JM, Tedeschi A, Schmitz J (2008) The cohesin complex and its roles in chromosome biology. *Gene Dev* **22:** 3089–3114

Petrinelli P, Antonelli A, Marcucci L, Dallapiccola B (1984) Premature centromere splitting in a presumptive mild form of Roberts syndrome. *Hum Genet* **66:** 96–99

Poser I, Sarov M, Hutchins JR, Heriche JK, Toyoda Y, Pozniakovsky A, Weigl D, Nitzsche A, Hegemann B, Bird AW, Pelletier L, Kittler R, Hua S, Naumann R, Augsburg M, Sykora MM, Hofemeister H, Zhang Y, Nasmyth K, White KP *et al* (2008) BAC TransgeneOmics: a high-throughput method for exploration of protein function in mammals. *Nat Methods* **5:** 409–415

Quivy JP, Roche D, Kirschner D, Tagami H, Nakatani Y, Almouzni G (2004) A CAF-1 dependent pool of HP1 during heterochromatin duplication. *EMBO J* **23:** 3516–3526

Resta N, Susca FC, Di Giacomo MC, Stella A, Bukvic N, Bagnulo R, Simone C, Guanti G (2006) A homozygous frameshift mutation in the ESCO2 gene: evidence of intertissue and interindividual variation in Nmd efficiency. *J Cell Physiol* **209:** 67–73

Rodriguez CI, Buchholz F, Galloway J, Sequerra R, Kasper J, Ayala R, Stewart AF, Dymecki SM (2000) High-efficiency deleter mice show that FLPe is an alternative to Cre-loxP. *Nat Genet* **25:** 139–140

Rowland BD, Roig MB, Nishino T, Kurze A, Uluocak P, Mishra A, Beckouet F, Underwood P, Metson J, Imre R, Mechtler K, Katis VL, Nasmyth K (2009) Building sister chromatid cohesion: Smc3 acetylation counteracts an antiestablishment activity. *Mol Cell* **33:** 763–774

Sakuno T, Watanabe Y (2009) Studies of meiosis disclose distinct roles of cohesion in the core centromere and pericentromeric regions. *Chromosome Res* **17:** 239–249

Schmitz J, Watrin E, Lenart P, Mechtler K, Peters JM (2007) Sororin is required for stable binding of cohesin to chromatin and for sister chromatid cohesion in interphase. *Curr Biol* **17:** 630–636

Schule B, Oviedo A, Johnston K, Pai S, Francke U (2005) Inactivating mutations in ESCO2 cause SC phocomelia and Roberts syndrome: no phenotype-genotype correlation. *Am J Hum Genet* **77:** 1117–1128

Skibbens RV, Corson LB, Koshland D, Hieter P (1999) Ctf7p is essential for sister chromatid cohesion and links mitotic chromosome structure to the DNA replication machinery. *Gene Dev* **13:** 307–319

Sutani T, Kawaguchi T, Kanno R, Itoh T, Shirahige K (2009) Budding yeast Wpl1 (Rad61)-Pds5 complex counteracts sister chromatid cohesion-establishing reaction. *Curr Biol* **19:** 492–497

Tomkins D, Hunter A, Roberts M (1979) Cytogenetic findings in Roberts-SC phocomelia syndrome(s). *Am J Med Genet* **4:** 17–26

Tomkins DJ, Sisken JE (1984) Abnormalities in the cell-division cycle in Roberts syndrome fibroblasts: a cellular basis for the phenotypic characteristics? *Am J Hum Genet* **36:** 1332–1340

Toth A, Ciosk R, Uhlmann F, Galova M, Schleiffer A, Nasmyth K (1999) Yeast Cohesin complex requires a conserved protein, Eco1p(Ctf7), to establish cohesion between sister chromatids during DNA replication. *Gene Dev* **13:** 320–333

Uhlmann F, Nasmyth K (1998) Cohesion between sister chromatids must be established during DNA replication. *Curr Biol* **8:** 1095–1101

Unal E, Heidinger-Pauli JM, Kim W, Guacci V, Onn I, Gygi SP, Koshland DE (2008) A molecular determinant for the establishment of sister chromatid cohesion. *Science* **321:** 566–569

Van Den Berg DJ, Francke U (1993) Roberts syndrome: a review of 100 cases and a new rating system for severity. *Am J Med Genet* **47:** 1104–1123

van der Lelij P, Godthelp BC, van Zon W, van Gosliga D, Oostra AB, Steltenpool J, de Groot J, Scheper RJ, Wolthuis RM, Waisfisz Q, Darroudi F, Joenje H, de Winter JP (2009) The cellular phenotype of Roberts syndrome fibroblasts as revealed by ectopic expression of ESCO2. *PLoS One* **4:** e6936

Vega H, Trainer AH, Gordillo M, Crosier M, Kayserili H, Skovby F, Uzielli ML, Schnur RE, Manouvrier S, Blair E, Hurst JA, Forzano F, Meins M, Simola KO, Raas-Rothschild A, Hennekam RC, Jabs EW (2010) Phenotypic variability in 49 cases of ESCO2 mutations, including novel missense and codon deletion in the acetyltransferase domain, correlates with ESCO2 expression and establishes the clinical criteria for Roberts syndrome. *J Med Genet* **47:** 30–37

Vega H, Waisfisz Q, Gordillo M, Sakai N, Yanagihara I, Yamada M, van Gosliga D, Kayserili H, Xu CZ, Ozono K, Jabs EW, Inui K, Joenje H (2005) Roberts syndrome is caused by mutations in ESCO2, a human homolog of yeast ECO1 that is essential for the establishment of sister chromatid cohesion. *Nat Genet* **37:** 468–470

Visel A, Carson J, Oldekamp J, Warnecke M, Jakubcakova V, Zhou X, Shaw CA, Alvarez-Bolado G, Eichele G (2007) Regulatory pathway analysis by high-throughput *in situ* hybridization. *PLoS Genet* **3:** 1867–1883

Wirth KG, Wutz G, Kudo NR, Desdouets C, Zetterberg A, Taghybeeglu S, Seznec J, Ducos GM, Ricci R, Firnberg N, Peters JM, Nasmyth K (2006) Separase: a universal trigger for sister chromatid disjunction but not chromosome cycle progression. *J Cell Biol* **172:** 847–860

Wu FM, Nguyen JV, Rankin S (2011) A conserved motif at the C terminus of sororin is required for sister chromatid cohesion. *J Biol Chem* **286:** 3579–3586

Yamagishi Y, Honda T, Tanno Y, Watanabe Y (2010) Two histone marks establish the inner centromere and chromosome bi-orientation. *Science* **330:** 239–243

Zhang JL, Shi XM, Li YH, Kim BJ, Jia JL, Huang ZW, Yang T, Fu XY, Jung SY, Wang Y, Zhang PM, Kim ST, Pan XW, Qin J (2008) Acetylation of Smc3 by Eco1 is required for S phase sister chromatid cohesion in both human and yeast. *Mol Cell* **31:** 143–151

Zink D (2006) The temporal program of DNA replication: new insights into old questions. *Chromosoma* **115:** 273–287

